Georgia State University
Center for High Angular Resolution Astronomy

The CHARA Michelson Array: A Kilometer-sized Optical/Infrared Interferometer

Astro 2020 Project White Paper:
Optical and Infrared Observations from the Ground

Douglas Gies, Theo ten Brummelaar, Gail Schaefer, Fabien Baron, and Russel White
CHARA, Department of Physics and Astronomy, Georgia State University,
P.O. Box 5060, Atlanta, GA 30302-5060 USA; gies@chara.gsu.edu

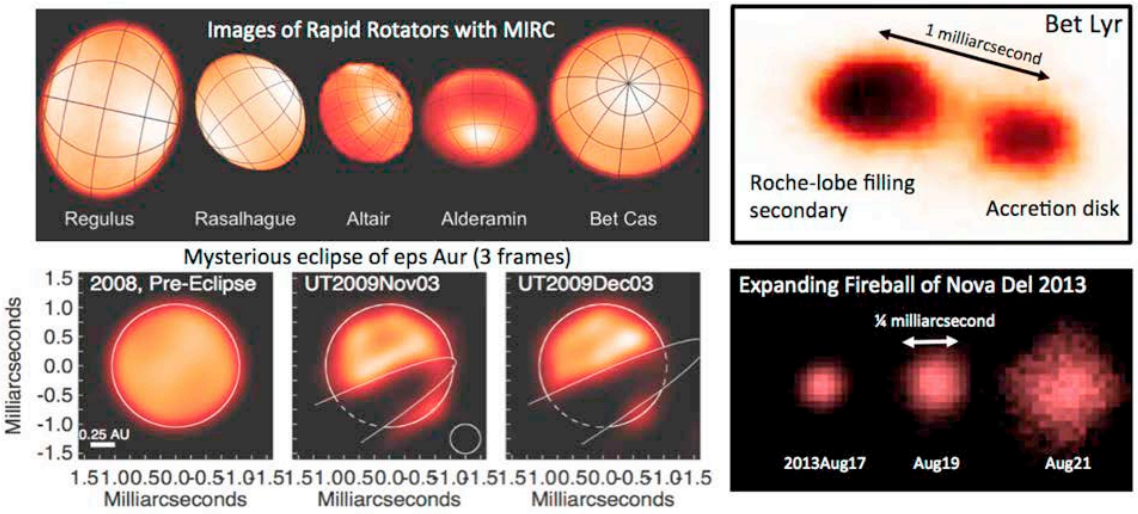

Images from the CHARA Array. Clockwise from upper left: Five rapid rotating stars showing oblate equatorial bulging; an image of the interacting binary star system β Lyrae directly showing Roche lobe distortion and mass exchange for the first time; the expansion of the fireball from the Nova Delphini 2013 thermonuclear eruption over a 4-day span; and, the passage of the dark disk surrounding an obscured star in front of the supergiant in the ε Aurigae eclipsing binary system.

1 Introduction

The quest in contemporary astronomy is to build telescopes to see ever fainter and smaller objects. The leading facilities pushing the high angular resolution barrier are the ESO Very Large Telescope Interferometer (VLTI) in Chile and the CHARA Array in the USA. The Georgia State University CHARA Array is located at Mount Wilson Observatory in southern California, and it consists of six 1 m telescopes in a Y-shaped configuration with baselines from 34 to 331 m in length. This remarkable facility measures objects over the angular size range from 0.3 to 40 milliarcsec (mas) using beam combiners in the optical and near-IR (0.5 to 2.2 microns). With its larger number of telescopes and longer baselines, it has four times the angular resolving power of VLTI (but less sensitivity), and this makes it the ideal facility to study the surfaces of stars in detail.

The CHARA Array has conducted scientific observations since 2004, and the 15 staff members support continuing upgrades (AO installation) and an observing program that now includes community access through the NOAO peer review system for 60 nights each year. There are now 184 referred publications[1] based upon Array data that include the following "firsts":

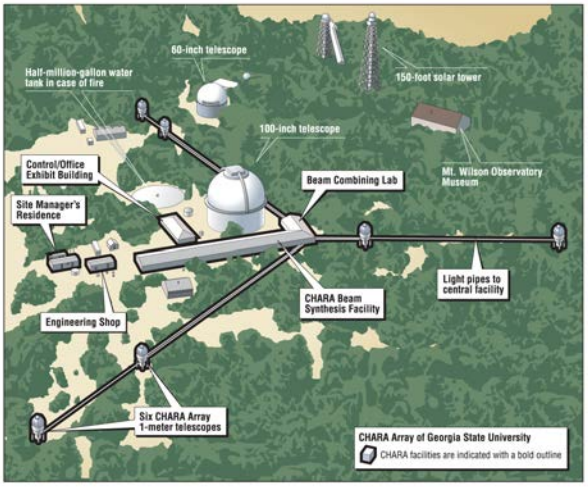

Fig. 1 – Layout of the CHARA Array.

- Gravity darkening on a star (α Leo)
- "*p*-factor" in the Baade-Wesselink method for Cepheids (δ Cep)
- Hot exozodiacal dust around a main-sequence star (Vega)
- Exoplanet stellar host diameter (HD 189733)
- Angular diameter for a halo population star (μ Cas A)
- Image of a single, main-sequence star (Altair)
- Image of an interacting binary (β Lyr)
- Shortest period binary yet resolved (α^2 CrB – 1.14 day)
- Image of a binary star system in eclipse (ε Aur)
- Earliest measurements of a nova diameter after eruption (Nova Del 2013)
- Images of starspots (λ And, ζ And)

These discoveries are re-invigorating stellar astrophysics, and they point the way forward to the kinds of investigations possible with better spatial dynamic range and sensitivity. Here we describe a new frontier facility, the CHARA Michelson Array (CMA) that will be built at Mount Wilson Observatory (MWO) and will be fully integrated into the existing infrastructure of the CHARA Array. The CMA will increase the resolving power 3×, the number of baselines 4×, and the sensitivity 4-10×. These performance jumps will open an enormous scope in astrophysical investigations, as illustrated by our primary science goals outlined below, and it will provide a focus for the nation's investment in the path towards extremely long baseline interferometers on the ground and in space.

[1] www.chara.gsu.edu/astronomers/journal-articles

2 Key Science Goals and Objectives

2.1 Imaging Stellar Surfaces

Map Starspots

The magnetic activity that is so well documented for the Sun is also found in starspots on the photospheres of other stars, and the existence of starspots is established through disk integrated measures of flux and magnetic strength. Now with the unprecedented resolution of the CHARA Array, starspots can be detected and mapped through interferometry (Roettenbacher et al. 2019). Roettenbacher et al. (2016) used the CHARA Array to map the starspots and their rotational motion across the magnetically active giant star ζ And. The star shows a persistent polar spot plus spots closer to the equator that appear and disappear on timescales of months. These properties indicate the action of a magnetic dynamo unlike that of the Sun. Such starspot maps offer us the means to test other methods of mapping such as Doppler imaging and light curve inversion (Roettenbacher et al. 2017). The greater resolution of the CMA will make possible measurements of spots and differential rotation spanning a range in stellar mass and age. This will place the Sun's magnetic activity into the larger context of stellar magnetism.

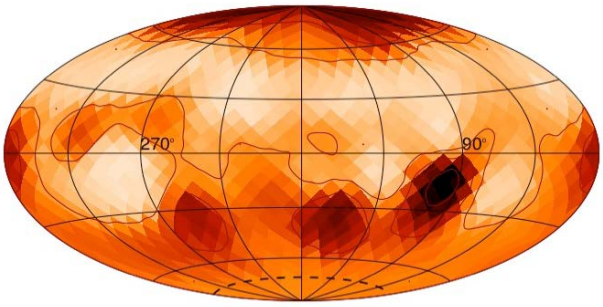

Fig. 2 – Starspot map for ζ And.

Track Convective Cells

Convection plays a dominant role in energy transport among cool, evolved stars, and 3D radiative hydrodynamic simulations indicate that large cells of hot, rising gas create long-lived, bright spots (Chiavassa et al. 2009). CHARA observations in the near-infrared show evidence of such bright spots among a number of nearby red supergiants (Baron et al. 2014). The higher resolution of the CMA will enable studies of such convective features among a range of cool stars and will determine cell lifetime, relation to rotation, and the connection between bright cells and asymmetric mass loss among the more luminous stars.

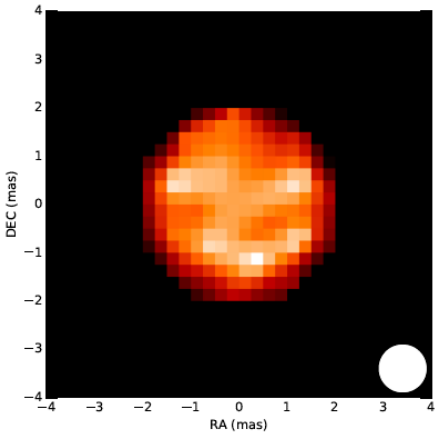

Fig. 3 – Cells on AZ Cyg (R. Norris, GSU).

Measure the Size and Shape of Extreme Stars

Interferometry is key to measurements of stellar size and shape (van Belle et al. 2019). The new capabilities of the CMA will allow us to measure faint cool dwarfs, distant hot stars, and young pre-main sequence stars (and study their contraction onto the main sequence). The CMA will measure angular sizes for all kinds of pulsating stars (Creech-Eakman et al. 2019) and provide important calibrations for asteroseismology relations (Huber et al. 2019). Imaging with the CMA will show the rotationally distorted shapes of rapid rotators (see cover page) to compare with simulations of rotating structures (Espinosa Lara & Rieutord 2013) and will reveal the variation in flux with co-latitude (gravity darkening) that is closely linked to their atmospheric properties.

2.2 Exoplanet Science

Make the First Resolved Image of an Exoplanet

Our goal is to track and image an exoplanet during a planetary transit (van Belle 2008; Chiavassa et al. 2014; Ligi et al. 2015). The silhouette image will reveal the planetary oblateness due to its rotation and show the orientation between the planetary spin and orbital axes (discussed in the context of light curve analysis by Pont et al. 2005). This work will show how the spin angular momentum of hot Jupiters compares to that of Jupiter and Saturn, and any misalignment will inform theories of planetary formation *in situ* or by violent migration (Naoz et al. 2011; Bailey & Batygin 2018). We calculated the interferometric visibility and phase as functions of projected baseline for the case of the transiting planet HD 189733b, which has angular diameters of 0.353 and 0.055 mas for the star and planet, respectively. The nominal expectation is that an object is fully resolved at the first zero in the visibility curve (Buscher 2015) for a baseline of $1.22\ \lambda / \theta =$ 2.7 km for the exoplanet observed at $\lambda = 0.6$ microns. However, our simulations show that the complex phase (measured by closure phase) is very sensitive to the details of the transit because of the large contrast, and the signal can be distinguished from that of spots in time series data. For example, the phase difference between models for a circular planet and one for the oblateness of Saturn (10%) amounts to as much as 15 degrees when measured in the third lobe of the visibility curve (around 1000 m in baseline), which is readily attained for instruments like the MIRC combiner at CHARA. Thus, the new CMA with kilometer baselines will be powerful enough to reconstruct images of the transiting exoplanets HD 189733b, HD 209458b, and GJ 436b, as well determining the transit trajectories of another 16 planets.

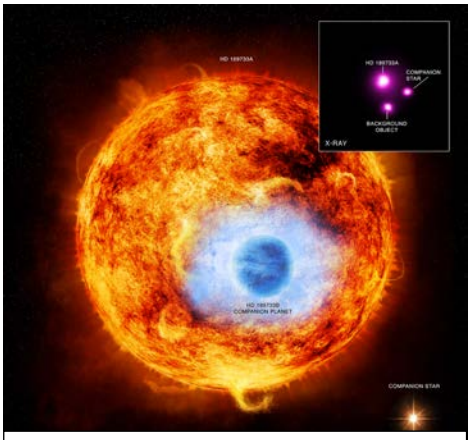

Fig. 4 – HD189733 (NASA/CXC).

Measure Radii of Transiting Exoplanet Host Stars

Photometric surveys from space will discover large numbers of transiting exoplanets. Missions such as the NASA TESS and ESA CHEOPS and PLATO satellites will provide thousands of new targets for study. Transit light curves yield the ratio of planetary to stellar radius, so the derivation of planetary radius relies on estimates of stellar radius. Interferometric measurements yield the stellar angular size that can be combined with a distance from GAIA to find the physical radius of the star, and hence the planet. The CMA will have the resolving power to measure angular diameters of solar-like stars out to a distance of 70 pc that will include hundreds of potential targets.

2.3 Explore Stellar Environments

Image the Disks Surrounding Young Stars

High angular resolution observations of newborn stars probe how mass accretion and mass loss lead to the formation of planets (Isella et al. 2019; Monnier et al. 2019; Weinberger et al. 2019). The gas and dust surrounding newborn stars is sculpted by hydrodynamical forces and gravitational forces of any embedded planets, so the geometry and spectra of the disk hold clues about young planetary systems. ALMA observations yield exquisite images of the cooler, outer dust emission, while near-IR interferometry probes the hotter, inner regions where terrestrial planet

formation occurs. CMA studies of nearby young systems will explore the influence of young planets and will detect their individual circumplanetary disks (Monnier et al. 2019).

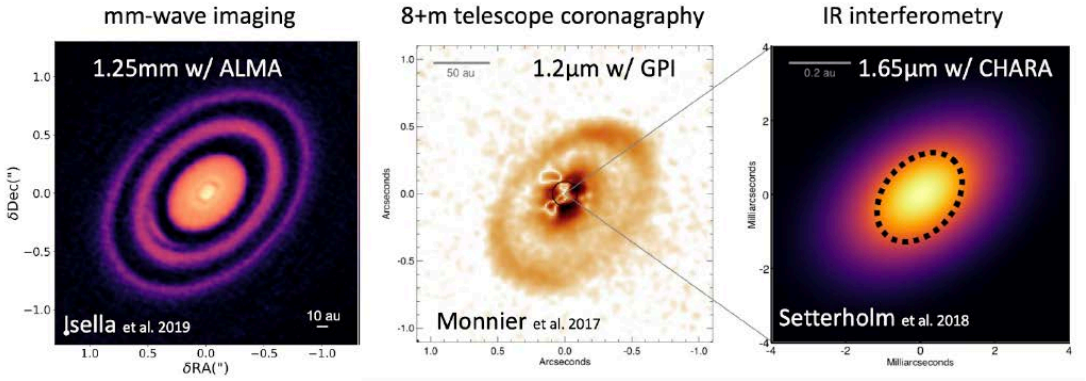

Fig. 5 – Multi-scale and multi-wavelength images of Herbig Ae star HD 163296.

Image Mass Loss from Evolved Stars

Stars approaching the end of their nuclear-burning lifetime become enormously luminous as they initiate processes that will ultimately drive away their outer layers to create a planetary nebula. During these late-life times, stars will experience expansion, convection, mixing, pulsation, and mass loss in a complex and inter-related way (Gies et al. 2019; Rau et al. 2019; Ridgway et al. 2019). Their winds accelerate over a distance of several to many radii, and a combination of spectral resolution and interferometry will enable a tomographic study of the acceleration zone. CMA observations will show how mass loss occurs for the radiatively-driven winds of hot stars and the dust-driven winds of cool stars, and how asymmetric structures may develop.

Explore the Interactions of Binary Stars

Binaries are the key to measuring masses and revealing how stars are transformed through mass transfer and loss (Breivik et al. 2019; Schaefer et al. 2019). Interferometry will reveal the workings of binary interactions from initial mass transfer (β Lyr, see cover) to complete loss of the donor's envelope and the spin-up of the mass gainer (ϕ Per; Fig. 6). CMA observations will have sufficient resolution to explore accretion and mass loss in the black hole binary Cygnus X-1 and to map the jet launching region of the microquasar SS 433. This will help us understand how such systems eventually become gravitational wave sources (Maccarone et al. 2019).

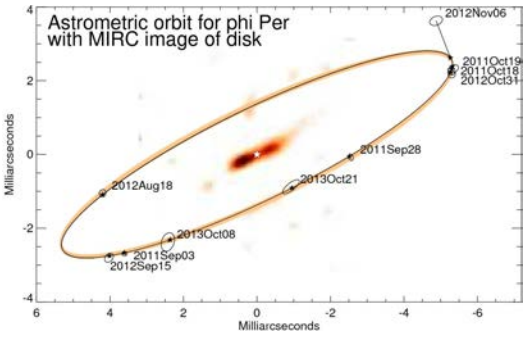

Fig. 6 – Orbit of the donor remnant in ϕ Per.

2.4 Respond to Rapid Transient Sources

The CMA will have the unique ability to explore the detailed spatial structure of time variable sources (Schaefer et al. 2019). CMA monitoring of cool flare stars will reveal the geometry and extent of bright flares. Triggered observations will follow micro-lensing sources, novae, and outbursts of Be stars and Luminous Blue Variables. A supernova in the local group would reach a magnitude and size within reach of CMA to observe the expansion rate and formation of structure.

2.5 Map the Inner Regions of Active Galactic Nuclei

The cores of AGN experience both accretion onto supermassive black holes and outflows that interact with the inner region of the host galaxies (Kishimoto et al. 2019). Interferometric measurements are beginning to resolve the innermost dusty, outflowing regions of nearby AGN. Observations with the CMA will attain a resolving power to map clearly this possibly "wind-launching" region, and even go beyond: start to isolate the putative accretion disk at the center for the first time. This will have important implications for studies of black hole masses, galaxy feedback, and AGN physics itself.

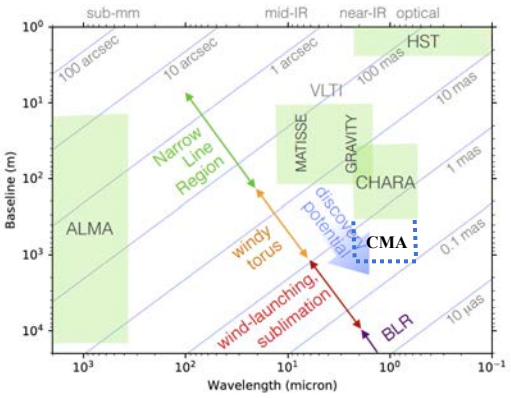

Fig. 7 – AGN discovery space.

3 Technical Overview of the CHARA Michelson Array

The transformative science capability of the 1 km baseline CHARA Michelson Array (CMA) is astonishing, and we are encouraged to pursue this path because of the success of the CHARA Array. We have a talented staff, we have made a significant investment in the infrastructure at Mount Wilson Observatory, and we have a supporting operating budget from the GSU College of Arts & Sciences. Here we describe the main components of the CMA that will consist of five new 2 m telescopes in an outer array and seven new 2 m telescopes replacing the current inner array.

3.1 General Requirements

The three main parameters driving the design of the CMA are: (1) wavelength range, (2) spatial dynamic range (angular resolution scales), and (3) sensitivity (telescope aperture). Additional parameters include the number of baselines (Section 3.2) and the spectral resolution (Section 3.5).

The working wavelength range will be from 0.6 to 2.2 microns. The short wavelength boundary is set by balancing the goals of very high angular resolution (that improves with shorter wavelength) and the use of adaptive optics for beam improvement (that becomes more difficult at shorter wavelength). The long wavelength limit is set by the need for measurements where cool objects are brighter and circumstellar gas and dust radiation contributions become significant in Young Stellar Objects and other objects with spatially extended emission (in a disk or outflow).

The main goal is to improve the angular resolution by a factor of three by building new baselines that are three times longer than the existing ones at the CHARA Array. Most of the key science goals require very high resolution, and in particular, the program to create an image of a transiting exoplanet (Section 2.2) requires baselines of about 1.0 km in order to record fringes in the "third lobe" of the visibility, i.e., at large spatial frequencies where the visibility and closure phase become sensitive to the detailed shape of the exoplanet. We have identified sites at MWO that will accommodate larger baselines (Section 3.2).

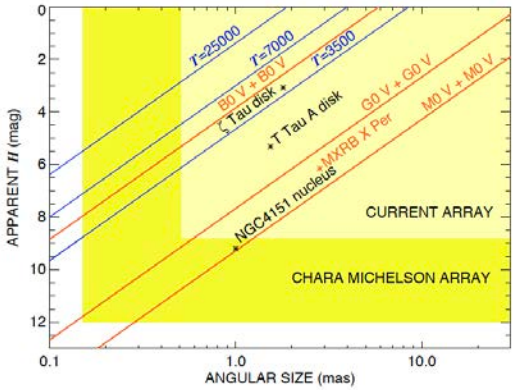

Fig. 8 – Range of CHARA Classic with sizes of stars, binaries (P=10 d), and key objects.

We need to increase the sensitivity by at least a factor of four. This can be achieved with 2 m aperture telescopes, high-order AO correction, and efficient fiber throughput. Better sensitivity will allow us to (1) resolve a large number of cool stars and AGN cores that are too faint for the current 1 m telescopes of the Array (Fig. 8), (2) attain sufficient S/N for fringe measurements at large spatial frequencies where the visibility itself is low, and (3) track on very red targets that have low flux in the visible where image tracking and wavefront sensor measurements are made. An example of the current CHARA Array limits in the *H*-band is shown in Figure 8, and a two-magnitude improvement will yield access to many kinds of cool stars, binary stars, and AGN cores.

3.2 Site and Telescopes

The ultimate goal for the CMA is to create a twelve-element interferometer consisting of seven telescopes in an inner array and five telescopes in an outer array. The inner array will be placed in the current location with the addition of a central telescope to improve (u,v) coverage and to implement baseline bootstrapping for better fringe tracking. The central telescope will dramatically improve our imaging capability and the phasing of the outer array. The potential ridge-top locations of the outer sites are indicated on a topographical map of Mount Wilson (Fig. 9). The west and southern locations are all close to paved roads, while the northern sites are close to a forest (unpaved) road. The maximum baselines are about 1080 m between the north – south pair and about 1130 m between the east – west pair. The inner and outer arrays will eventually operate together to create a network of $N(N-1)/2 = 66$ telescope pairs, resulting in a four-fold increase in our sampling of spatial frequencies. All the sites are located within the San Gabriel Mountains National Monument managed by the U.S. Forest Service.

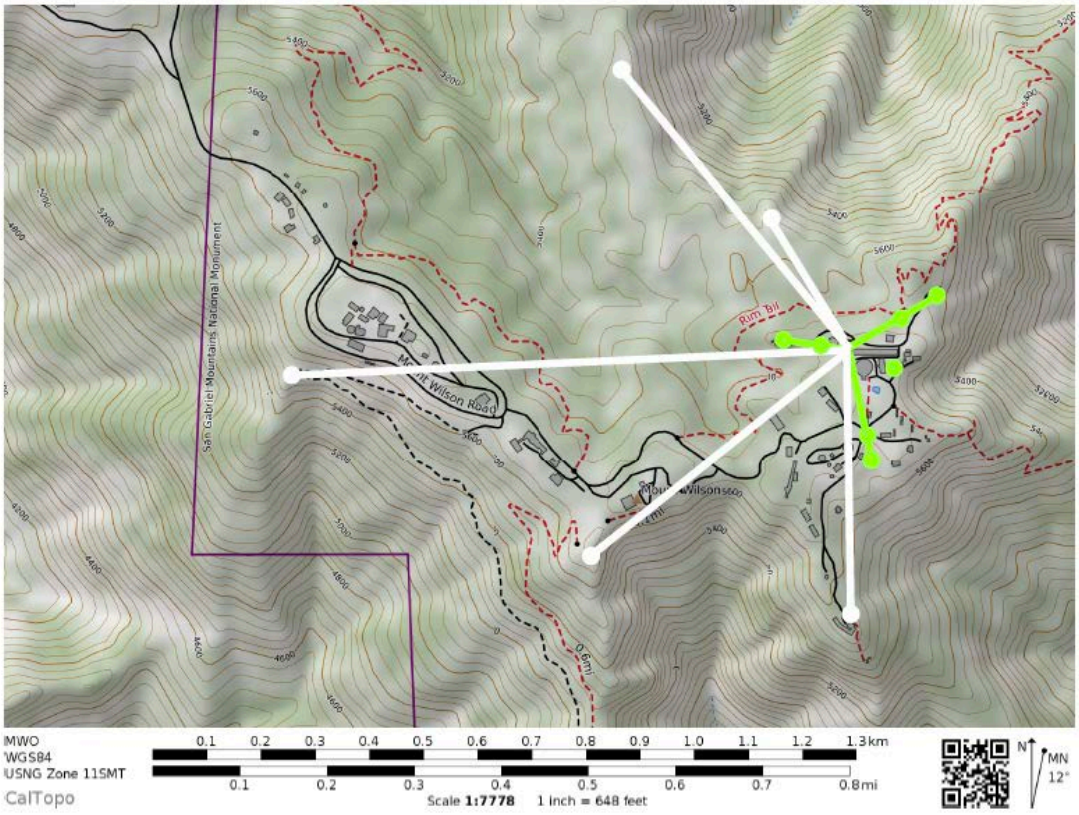

Fig. 9 – Configuration of the outer (white) and inner (green) arrays.

Each telescope will be placed in an elevated enclosure to avoid ground-seeing issues, and the telescopes will be supported on alti-azimuth mounts. The telescopes will have 2 m, light-weight primaries that are large enough to meet sensitivity requirements, but still small enough to be easily transported and inserted into the existing aluminization chamber in the 100-inch telescope building at MWO. The optical design is not set, but it will be relatively simple because of the very small field-of-view of the interferometer. Each telescope will be equipped with high-order adaptive optics (AO) systems to remove atmospheric distortions and improve fiber injection efficiency.

3.3 Beam Transport

We will use two methods to relay light from each telescope to the central, existing beam combination laboratory (BCL). The first is to use a set of fiber optic cables to connect each telescope to the BCL following the example of the ‘OHANA Iki project at the Mauna Kea Observatory that successfully created fringes from a pair of telescopes using 300 m long fibers (Woillez et al. 2017). These same fiber cables are now being tested at CHARA for telescope linkage for the ALOHA experiment for *L*-band interferometry (Lehmann et al. 2019b). There are now available many kinds of single-mode fibers that have relatively low propagation losses and that work well in the optical and near-infrared bands (Labadie et al. 2016), and we plan to have several sets that are optimized for specific wavelength bands. Secondly, the seven telescopes of the inner array will relay light either by fibers and/or by the existing partially evacuated light pipes along the line of sight (ten Brummelaar et al. 2005), as applications require.

3.4 Optical Path Delay

All the optical fibers have the same length in order to balance their inherent chromatic dispersion, so the delay required to match wavefronts from different telescopes is due to the offset of the target from the zenith. We plan to send the fiber output to the current Optical Path Length Equalization (OPLE) building (Beam Synthesis Facility in Fig. 1), where path length differences are introduced in both fixed lengths and real-time moving rail carts that run along a 43 m stretch of the building. There is room in the building for two additional rails beyond the current six beams, and these will be extended into a section currently used for storage to obtain a full 70 m of variable delay. The maximum rate of change of delay amounts to about 70 mm/sec for a 1 km east – west baseline, and with a double-pass system of cart reflections we should obtain at least one hour of continuous observations with the variable delay system before needing to change the amount of fixed delay. Thus, the existing OPLE building will be adequate for the enlarged dimensions of the outer array.

3.5 Beam Combiners

Mode	# Telescopes	Band	Spectral Res.	Origin
CLASSIC	2	*JHK*	Broad band	GSU
CLIMB	3	*JHK*	Broad band	GSU
MIRCX	6	*H*	50	Exeter /Michigan
MYSTIC	6	*K*	50+	Michigan
PAVO	2	630-900nm	30	Sydney/ANU
VEGA	2-3	480-850nm	6000	Nice
SPICA	6	600-900nm	300/3000	Nice

The Beam Combination Laboratory at CHARA hosts five different beam combiners and two more are under construction: MYSTIC (Monnier et al. 2018b) and SPICA (Mourard et al. 2018). These provide a diverse selection of number of telescopes included, wavelength coverage, spectral resolution, and limiting magnitude. The CMA will work with all of these using a maximum subset of eight telescopes for the eight beams in the OPLE, and we anticipate that new combiners based upon Integrated Optics concepts will be built in the future. We are also planning to feed light from the four unused telescopes to a high-resolution spectrograph for simultaneous investigations.

4 Technology Drivers

The success of the operating systems at the CHARA Array demonstrates that the basic technologies are already in place to build the CMA. There are several areas of development that we are investigating that will influence the final efficiency and sensitivity of the CMA.

The new telescopes will need high order AO systems to deal with atmospheric turbulence and produce a well-conditioned beam for transmission. We are currently installing deformable mirrors in the light path of the CHARA Array telescopes for this purpose, and initial results indicate that the AO systems deliver a significant improvement in light throughput and sensitivity (ten Brummelaar et al. 2018). The integration of AO on the CHARA Array will offer valuable lessons on the best approaches for AO incorporation into the new CMA telescopes. We are studying ways to optimize beam injection into optical fibers (Mourard et al. 2018), we have developed prototypes of fiber-based optical combiners (Lehmann et al. 2019b; Martinod et al. 2018), and we have found techniques to stabilize long fiber optic cables for interferometry (Lehmann et al. 2019a). This expertise will help serve to characterize the losses, chromatic dispersion, and birefringent properties of available fibers for use at the CMA.

Another area for development is the concept for the expanded delay lines (Section 3.4). With longer baselines, the length of the variable delay part of the system is the limiting factor for the available tracking time between changes in fixed delay, and we need to maximize the variable delay for efficient operations. Several concepts will be developed and a design set in the near future. The focus on fainter targets will require a fringe tracking system for longer exposures such as the SPICA-FT system now being developed (Mourard et al. 2018).

5 Organization, Partnerships, and Current Status

The CHARA Array is owned and operated by Georgia State University, and GSU will take the leadership role in building the CMA. CHARA operates at MWO under a site use agreement with the Mount Wilson Institute on behalf of the Carnegie Observatories, who hold a long-term lease from the U.S. Forest Service. Building the CMA will require the support of all these stake-holders. The CHARA Array is operated by a talented staff of 15 members led by the CHARA Array Director, Dr. Theo ten Brummelaar. CHARA is a center in the GSU College of Arts and Sciences and is led by Regents' Professor Douglas Gies. The CHARA consortium consists of scientists who make vital contributions in instrumentation and other support, and it includes NOAO, Univ. of Michigan, Univ. of Exeter (UK), l'Observatoire de Paris, l'Observatoire de la Côte d'Azur, Univ. de Limoges, Sydney Univ., Australian National Univ., and Kyoto Univ. The activities of

the consortium are documented by the reports and papers hosted on our web site[2]. The CHARA Array is used for astronomical observing every night excluding ten weeks during the winter when conditions are poor. Time is allocated to consortium members through an internal Telescope Allocation Committee. Time is also awarded to the community at large through competitive proposals to the NOAO peer review system for some 60 nights/year.

6 Schedule

Phase 1 (Years 1, 2):

- Appraisal of available optical fibers.
- Build a two-telescope fiber system and a prototype fiber injector system.
- Determine telescope design specifications.
- Identify and prepare sites for the outer array telescopes.
- Design additions for the delay lines in the OPLE building.
- Develop a plan for a revised beam switchyard (connecting OPLE and BCL).

Phase 2 (Years 3, 4, 5):

- Build and install five new outer array telescopes and their enclosures.
- Build and install fiber conduits to the OPLE building.
- Install new delay lines and rebuild the beam switchyard.
- Develop software for the telescope and delay line control systems.
- Begin observations with the outer array.

Phase 3 (Years 6, 7, 8):

- Replace the six existing 1 m telescopes of the inner array with seven 2 m telescopes.
- Build and install a fiber optics conduit system for the inner array telescopes.
- Design a 12-telescope operating system for beam combinations of any telescope pair.
- Develop concepts for new beam combiners utilizing the full eight beams.
- Begin observations with the combined inner and outer arrays.

Phase 4 (Years 9 - 28):

- Routine science observations.

7 Cost Estimates

We created a preliminary budget (06/19/2019) based upon our current annual operating costs for the CHARA Array and applying a 3% per year rate of salary increases (the historical average at GSU over the last decade). We also assumed a start date in FY21 (07/01/2020) when the GSU fringe benefit rate is 35% and the indirect cost (IDC) rate is 55.5%; in subsequent years the IDC rate will be 56.0%. The IDC is not applied to equipment over $5000. The cost estimates are summarized in the table below for the different project phases (Section 6) and for operational and capital costs. The total cost is estimated to be $102M over eight years.

[2] www.chara.gsu.edu/news/meetings

Project Phase	Year #	Personnel/Operations	Capital Costs	Total
1	1-2	$ 5.4M	$ 0.5M	$ 5.9M
2	3-5	$ 8.6M	$33.6M	$42.2M
3	6-8	$ 9.4M	$44.4M	$53.8M
Total		$23.4M	$78.5M	**$101.9M**

Column 3 lists the operational costs that are dominated by staff salaries. The amounts are based upon the current salaries of 15 CHARA staff members plus three additional staff (project manager and two engineers). This staffing level will allow us to continue to act as a national facility and to offer community access to the Array (and then CMA) through NOAO. The operations costs also include an annual site fee paid to the Mount Wilson Institute, internet costs, and general maintenance costs ($100K per year). We expect that once CMA is fully operational, the annual operations costs will continue to run about $2.4M per year for support of community access.

The capital (one time) costs are summarized in column 4. About 61% of these costs are associated with the purchase of the telescopes. We estimate that the cost will be about $4M per telescope based upon the current cost for a 1.5 m telescope from PlaneWave Instruments ($2M) and upon the typical scaling relation between aperture and cost. However, we are exploring novel thin mirror systems that might substantially reduce telescope costs. The other major capital costs are the telescope enclosures (12×$400K), the AO and fiber injection systems (12×$500K), and the delay line construction ($1M). We added a 25% contingency amount at this early stage.

We anticipate that the operating costs will continue to be funded through NSF grants, the GSU College of Arts and Sciences (currently $619K per year), and contributions from the CHARA consortium partners. We are planning to seek funding for the capital costs through grants from NSF and the State of Georgia, and through foundation and private fund-raising activities by GSU.

8 Conclusions

The CHARA Array has proven to be an effective and innovative tool for stellar astrophysics, and the next stage of work with the CMA will open up a vast range of investigations at the 100 micro-arcsec level. The CMA will enable breakthroughs in stellar imaging, exoplanet research, and in exploration of circumstellar environments. It will provide the resolution to measure sizes of the distant massive stars and it will have the sensitivity to measure the fainter nearby and cooler stars, extending our understanding at both ends of the stellar mass range. It will have numerous other applications in studies of time-variable objects (gravitational lenses, novae, supernovae) and of the cores of Active Galactic Nuclei. The resolving power of the CMA will be an order of magnitude better than that of the ESO VLTI that is limited to smaller baselines and near-IR wavelengths. The new CMA interferometer will be a national resource available to astronomers through the NOAO peer review system for 100-150 nights per year. It will spur the growth of interest and expertise in interferometry and provide a focus for the training of a new generation of astronomers who will build future instruments in space and on the ground (The Planet Formation Imager; Monnier et al. 2018a). Albert Michelson made the first measurement of the stellar sizes at Mount Wilson Observatory, and it is fitting that his namesake CHARA Michelson Array will take Mount Wilson Observatory into the next decades of exploration of stellar surfaces and their surroundings.

References

Bailey, E., & Batygin, K. 2018, ApJ, 866, L2
Baron, F., Monnier, J. D., Kiss, L. L., et al. 2014, ApJ, 785, 46
Breivik, K., Price-Whelan, A. M., D'Orazio, D. J., 2019, arXiv:1903.05094
Buscher, D. F. 2015, Practical Optical Interferometry, Imaging at Visible and Infrared Wavelengths (Cambridge, UK: Cambridge University Press)
Chiavassa, A., Ligi, R., Magic, Z., et al. 2014, A&A, 567, A115
Chiavassa, A., Plez, B., Josselin, E., et al. 2009, A&A, 506, 1351
Cowan, N. B., Machalek, P., Croll, B., et al. 2012, ApJ, 747, 82
Creech-Eakman, M. J., Ridgway, S., Guzik, J., et al. 2019, BAAS, 51 (3), 196
Espinosa Lara, F., & Rieutord, M. 2013, A&A, 552, A35
Gies, D., Owocki, S. P., Ridgway, S., & ten Brummelaar, T. 2019, BAAS, 51 (3), 171
Huber, D., Basu, S., Beck, P., et al. 2019, BAAS, 51 (3), 488
Isella, A., Richi, L., Andrews, S. M., et al. 2019, BAAS, 51 (3), 174
Kishimoto, M., ten Brummelaar, T., Gies, D., et al. 2019, BAAS, 51 (3), 156
Labadie, L., Berger, J.-P., Cvetojevic, N., et al. 2016, Proc. SPIE, 9907, 990718
Lehmann, L., Delage, L., Grossard, L., et al. 2019a, Exp. Astr., online first, https://doi.org/10.1007/s10686-019-09627-x
Lehmann, L., Grossard, L., Delage, L., et al. 2019b, MNRAS, 485, 3595
Ligi, R., Mourard, D., Lagrange, A.-M., Perraut, K., & Chiavassa, A. 2015, A&A, 574, A69
Maccarone, T. J., Chomiuk, L., Miller-Jones, J., et al. 2019, BAAS, 51 (3), 226
Martinod, M. A., Mourard, D., Bério, P., et al. 2018, A&A, 618, A153
Monnier, J. D., Harries, T. J., Aarnio, A., et al. 2017, ApJ, 838, 20
Monnier, J. D., Kraus, S., Ireland, M. J., et al. 2018a, Exp. Astr., 48, 517
Monnier, J. D., Le Bouquin, J.-B., Anugu, N., et al. 2018b, Proc. SPIE, 10701, 1070122
Monnier, J., Rau, G., Sanchez-Bermudez, J., et al. 2019, BAAS, 51 (3), 498
Mourard, D., Nardetto, N., ten Brummelaar, T., et al. 2018, Proc. SPIE, 10701, 1070120
Naoz, S., Farr, W. M., Lithwick, Y., Rasio, F. A., & Teyssandier, J. 2011, Nature, 473, 187
Pont, F., Gilliland, R. L., Moutou, C., et al. 2005, A&A, 476, 1347
Rau, G., Montez, R., Jr., Carpenter, K., et al. 2019, BAAS, 51 (3), 241
Ridgway, S., Akeson, R., Baines, E., et al. 2019, BAAS, 51 (3), 332
Roettenbacher, R. M., Norris, R. P., Baron, F., et al. 2019, BAAS, 51 (3), 181
Roettenbacher, R. M., Monnier, J. D., Korhonen, H., et al. 2016, Nature, 533, 217
Roettenbacher, R. M., Monnier, J. D., Korhonen, H., et al. 2017, ApJ, 849, 120
Schaefer, G. H., Casan, A, Klement, R., et al. 2019, BAAS, 51 (3), 502
Schaefer, G. H., Duchêne, G., Farrington, C. D., et al. 2019, BAAS, 51 (3), 483
Setterholm, B. R., Monnier, J. D., Davies, C. L., et al. 2018, ApJ, 869, 164
ten Brummelaar, T. A., McAlister, H. A., Ridgway, S. T., et al. 2005, ApJ, 628, 453
ten Brummelaar, T. A., Sturmann, J., Sturmann, L., et al. 2018, Proc. SPIE, 10703, 1070304
van Belle, G. T. 2008, PASP, 120, 617
van Belle, G., Baines, E., Boyajian, T., et al. 2019, BAAS, 51 (3), 381
Weinberger, A. J., Turner, N., Hasegawa, Y., et al. 2019, BAAS, 51 (3), 445
Woillez, J., Lai, O., Perrin, G., et al. 2017, A&A, 602, A116
Zhao, M., Monnier, J. D., Che, X., et al. 2011, PASP, 123, 964